coatings

MDPI

Article

Thermal Aging-Induced Alterations in Surface and Interface Topography of Bio-Interactive Dental Restorative Materials Assessed by 3D Non-Contact Profilometry

Zehra Güner [1,*], Gökçe Keçeci [2], Sadık Olguner [3], Hakan Çandar [3], Ayşenur Güngör Borsöken [4] and Lezize Sebnem Turkun [5]

[1] Department of Paediatric Dentistry, Faculty of Dentistry, Gaziantep University, Gaziantep 27310, Türkiye
[2] Department of Prosthodontic Dentistry, Faculty of Dentistry, Kahramanmaraş Sütçü Imam University, Kahramanmaraş 46040, Türkiye
[3] Department of Mechanical Engineering, Engineering Faculty, Gaziantep University, Gaziantep 27310, Türkiye; olguner@gantep.edu.tr (S.O.)
[4] Department of Restorative Dentistry, Faculty of Dentistry, Gaziantep University, Gaziantep 27310, Türkiye
[5] Department of Restorative Dentistry, Faculty of Dentistry, Ege University, Izmir 35040, Türkiye; sebnemturkun@gmail.com
* Correspondence: zsivgan@gmail.com; Tel.: +90-5512502633

Highlights

What are the main findings?

- Surface roughness changes varied among the restorative materials evaluated and thermal aging increased the areal surface roughness (Sa) of all tested restorative materials.
- Interface regions (enamel/material and cement/material) showed higher roughness values than material surfaces.

What are the implications of the main findings?

- 3D non-contact profilometry enabled detailed assessment of surface and interface topography.
- The glass-hybrid restorative system with protective coating exhibited a different roughness pattern compared with other materials.

Abstract

This study aimed to evaluate the effects of thermal cycling and restorative material type on surface roughness of material surfaces and dental interfaces using a non-contact profilometer. Ninety Class V cavities (2 mm × 4 mm × 2 mm in height, width, and depth) were prepared on extracted third molars and restored with four bio-interactive materials (Equia Forte, Cention-N, Activa BioActive Restorative, Fuji II LC) and one composite resin (Solare-X) (n = 18/group). After polishing (Optidisc), initial surface roughness (Sa, µm) was measured following 24 h immersion in distilled water. Measurements were performed at cement/material (400 × 1600 µm^2), enamel/material (1600 × 400 µm^2), and material surfaces (800 × 800 µm^2). Samples underwent 10,000 thermal cycles (5–55 °C) to simulate aging, and roughness was re-measured. Data were analyzed with two-way repeated measures ANOVA and Tukey's post hoc test ($p < 0.05$). Solare-X showed the lowest roughness, while Fuji II LC and Activa BioActive Restorative were smoother than Cention-N and Equia Forte ($p < 0.01$). All materials exhibited significant roughness increases after thermal cycling ($p < 0.01$). Cement/material and enamel/material interfaces consistently showed higher roughness than material surfaces ($p < 0.01$). Thermal cycling significantly increased surface roughness of all tested materials. Interfaces demonstrated greater roughness than

Check for updates

Academic Editor: Seunghan Oh

Received: 4 December 2025
Revised: 26 December 2025
Accepted: 29 December 2025
Published: 3 January 2026

Copyright: © 2026 by the authors. Licensee MDPI, Basel, Switzerland. This article is an open access article distributed under the terms and conditions of the Creative Commons Attribution (CC BY) license.

material surfaces, indicating higher susceptibility to plaque retention and potential risk for long-term restoration success.

Keywords: bio-interactive materials; dental tissue interfaces; non-contact profilometer; surface roughness; thermocycling

1. Introduction

Restorative materials in dentistry are intended to restore the functional, aesthetic, and biological properties of teeth [1]. Resin-based materials are widely used, particularly in cervical lesions, due to their adhesive capability and favorable esthetics [2]. However, despite their clinical success, resin composites present several limitations, including technique sensitivity, polymerization shrinkage, degradation of interfacial adhesion over time, and susceptibility to secondary caries and periodontal incompatibility [3,4]. In addition, many conventional resin composites exhibit limited buffering capacity and lack intrinsic antibacterial properties, conditions that may favor the development of acidogenic biofilms and increase caries risk at the restoration margins [5,6]. Although certain conventional or newly developed resin-based materials may release fluoride ions depending on their formulation, this characteristic alone is generally insufficient to ensure sustained pH regulation or biologically meaningful interaction at the material–tissue interface.

In response to these limitations, contemporary restorative strategies have focused on the development of materials described as “bioactive” or “bio-interactive” which aim to interact with biological processes in addition to restoring tooth structure. According to Hench, bioactive materials are defined as those capable of eliciting specific biological responses at the material–tissue interface, resulting either in the formation of an apatite-like surface layer in the presence of water contained in biological tissues or in the establishment of a direct bond with surrounding tissues [7,8]. Materials such as mineral trioxide aggregate and Biodentine meet this definition by forming hydroxyapatite following hydrolysis of calcium- and phosphate-based components when exposed to tissue fluids [9–11]. However, most restorative materials currently used in dentistry do not fully satisfy the criteria for true bioactivity. Instead, they are more appropriately classified as bio-interactive, as their interaction with dental tissues predominantly occurs through ion release rather than direct initiation of mineralization [5]. For this reason, glass ionomer cements, resin-modified glass ionomer cements, and certain hybrid restorative materials are commonly evaluated within the bio-interactive category, particularly in the context of minimally invasive dentistry, where ion exchange at the material–tissue interface plays a biologically relevant role [12–14].

Glass ionomer cements (GICs) are classified as bio-interactive materials because they release therapeutic ions such as fluoride, calcium, and strontium, supporting remineralization processes. Their biological behavior is influenced not only by ion release but also by surface characteristics and pH modulation [5,14,15]. Due to their limited mechanical strength in high-stress areas, modified formulations such as high-viscosity and resin-modified glass ionomer cements have been developed to improve clinical performance [16]. Equia Forte HT is a high-viscosity glass ionomer-based glass hybrid material used with a light-cured resin coating that alters surface characteristics [17]. Resin-modified glass ionomers, such as GC Fuji II LC, incorporate resin components into the glass ionomer matrix and exhibit fluoride release that decreases over time [18,19]. In addition, alkasite materials like Cention N and injectable bio-interactive materials such as Activa BioActive Restorative release various ions that may contribute to pH modulation and ion exchange at the tooth–material interface [20–22].

Despite advancements in restorative materials, surface roughness remains a clinically relevant concern. Increased surface roughness has been associated with plaque accumulation, gingival inflammation, secondary caries, discoloration, and reduced wear resistance [23–25]. Smoother restoration surfaces are associated with improved esthetics, reduced plaque retention, and better periodontal compatibility [26–28]. Surface roughness can be assessed using profilometric techniques, including contact (mechanical) and non-contact (optical) methods [29]. Mechanical profilometry, which employs a diamond stylus, may be limited by tip size and potential surface damage [30–32]. In contrast, optical profilometry enables three-dimensional, non-contact surface evaluation, allowing more accurate assessment of true surface topography [33,34].

Areal surface roughness parameters such as Sa and Sz, defined under ISO 25178–2:2019, provide more reliable three-dimensional surface characterization than traditional two-dimensional parameters such as Ra [35,36]. Sa represents the arithmetic mean height deviation calculated from the surface height distribution after subtraction of the least-squares reference plane.

Marginal adaptation is another critical determinant of long-term restorative success. Marginal discrepancies may lead to leakage, water sorption, and eventual restoration failure [37,38]. Intraoral conditions, including temperature fluctuations, saliva, and pH changes, expose restorative materials to thermal stress, which may alter surface characteristics and interfacial integrity over time [25,39–41]. Thermal cycling is widely used as an in vitro method to simulate intraoral thermal stress and aging [42,43]. According to ISO TR 11450 (1994), 10,000 thermal cycles correspond approximately to one year of clinical service [44]. Thermal aging may contribute to degradation at the material–tooth interface, potentially affecting surface roughness and marginal adaptation [43–45].

The literature addressing the effect of thermal cycling on surface roughness at restorative material surfaces and at enamel/material and cement/material interfaces remains limited. Therefore, the aim of this in vitro study was to evaluate the effect of thermal aging simulating one year of intraoral use on the surface roughness of restorative materials, as well as enamel/material and cement/material interfaces.

The null hypotheses tested were:

(1) Thermal aging has no significant effect on the surface roughness of different restorative materials.
(2) Thermal aging has no significant effect on the surface roughness of restorative material–enamel interfaces.
(3) Thermal aging has no significant effect on the surface roughness of restorative material–cement interfaces.

2. Materials and Methods

The a priori power analysis was performed with GPower 3.1. Assuming a fixed-effects one-way ANOVA with five groups, an α level of 0.05 (two-tailed), power (1–β) of 0.80, and an effect size of Cohen's f = 0.50 [46], the required total sample size was n = 90 (n = 18 per material group) *.

2.1. Sample Preparation

In this study, 90 impacted third molar teeth without cracks, discoloration, and a single crown, extracted within 3 months at the Gaziantep University Faculty of Dentistry, Department of Oral and Maxillofacial Surgery, were used. Only teeth extracted for therapeutic purposes as part of routine dental treatment were used, and all patients had previously signed informed consent forms. LED-illuminated dental loupes (Binocular, Keeler Ltd., Windsor, UK) were used to detect possible cracks/defects in the teeth. After extraction, the

teeth were immersed in 0.1% thymol solution for one week to disinfect and remove any remaining organic and inorganic materials, and then in distilled water at room temperature until the time of measurement to prevent dehydration [25]. All the specimens were prepared at the Department of Pediatric Dentistry, Gaziantep University School of Dentistry. The current study had the approval of the Gaziantep University Non-Interventional Ethics Committee (No. 2024/325). For cavity preparation, a high-speed handpiece (SUPERtorque, KaVo Dental GmbH, Biberach, Germany) under water cooling was used. Class V cavities were prepared on the buccal surfaces of the teeth with a green-belted fissure bur [801-010 Medium diamond (MDT FG Diamond NorthAfula, Israel)]. Cavities were prepared using a matrix tape key template, and cavity depth was controlled by a marked periodontal probe [43]. Cavity dimensions were standardized as 2 mm in occluso-gingival height, 4 mm in mesiodistal width, and 2 mm in depth, as illustrated in Figure 1. A 2 mm bevel was prepared on the occlusal margin, and the gingival margin was positioned precisely at the enamel–cement junction. To ensure preparation consistency, the diamond burs were replaced after every five cavity preparations.

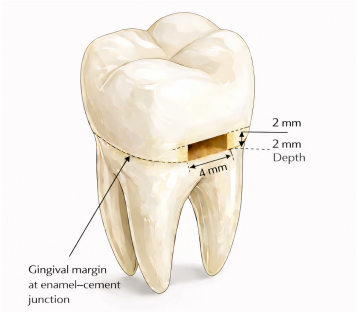


Figure 1. Schematic illustration of a standardized Class V cavity preparation on a molar tooth.

Five groups of bio-interactive materials were tested. The properties, composition and manufacturers of the used bio-interactive materials used were shown in Table 1. The teeth were randomly assigned to these groups and restored with the following materials (n = 18):

Group 1: EQUIA Forte (EF); GC, Tokyo, Japan

Group 2: Cention-N (CN); Ivoclar, Schaan, Liechtenstein

Group 3: Activa BioActive Restorative (AB); Pulpdent, Watertown, MA, USA

Group 4: Fuji II Light Cure (F); GC, Tokyo, Japan

Group 5: Solare-X (SX); GC, Tokyo, Japan.

Preparation of the samples according to different groups:

The methodology of sample preparation and surface roughness measurements are shown in Figure 2.

Table 1. Bio-interactive dental materials used in the study and their formulations.

Materials	Type	Compositions	Manufacturer	LOT Numbers
Equia Forte (EF)	High-viscosity glass ionomer cement	Powder: 95 wt.% strontium fluoroaluminosilicate glass, 5 wt.% polyacrylic acid Liquid: 40 wt.% aqueous polyacrylic acid EQUIA Forte Coat: 40–50 wt.% methyl methacrylate, 10–15 wt.% colloidal silica, 0.09 wt.% camphorquinone, 30–40 wt.% urethane methacrylate, 1–5 wt.% phosphoric ester monomer	GC, Tokyo, Japan	2307251

Table 1. *Cont.*

Materials	Type	Compositions	Manufacturer	LOT Numbers
Activa BioActive Restorative (AB)	Bio-interactive Restorative Material	Blend of diurethane and other methacrylates with modified polyacrylic acid (44.6 wt.%), amorphous silica (6.7 wt.%), sodium fluoride (0.75 wt.%); approximately 56 wt.% reactive glass particles in a patented rubberized resin matrix	Pulpdent, Watertown, MA, USA	210324
Cention-N (CN)	Dual cure bulk-fill composite	Liquid: Dimethacrylates, initiators, stabilizers, additives, flavoring agents Powder: Calcium fluorosilicate glass, barium glass, calcium–barium–aluminum fluorosilicate glass, isofillers, ytterbium trifluoride, initiators, pigments; total inorganic filler content: 78.4 wt.% (particle size: 0.1–7 µm)	Ivoclar, Schaan, Liechtenstein	Z0233Y
Fuji II (F)	Resin-modified glass ionomer cement	Liquid: Polyacrylic acid Powder: Al_2O_3–SiO_2–CaF_2 glass and HEMA urethane dimethacrylate	GC; Tokyo, Japan	2302133
Solare-X (SX)	Composite Resin (Nanofilled)	UDMA-based dimethacrylate resin matrix; silica nanoparticles, fluoroaluminosilicate glass fillers, and prepolymerized fillers; total inorganic filler content: 77 wt.% (mean particle size: 0.85 nm)	GC, Tokyo, Japan	1902071

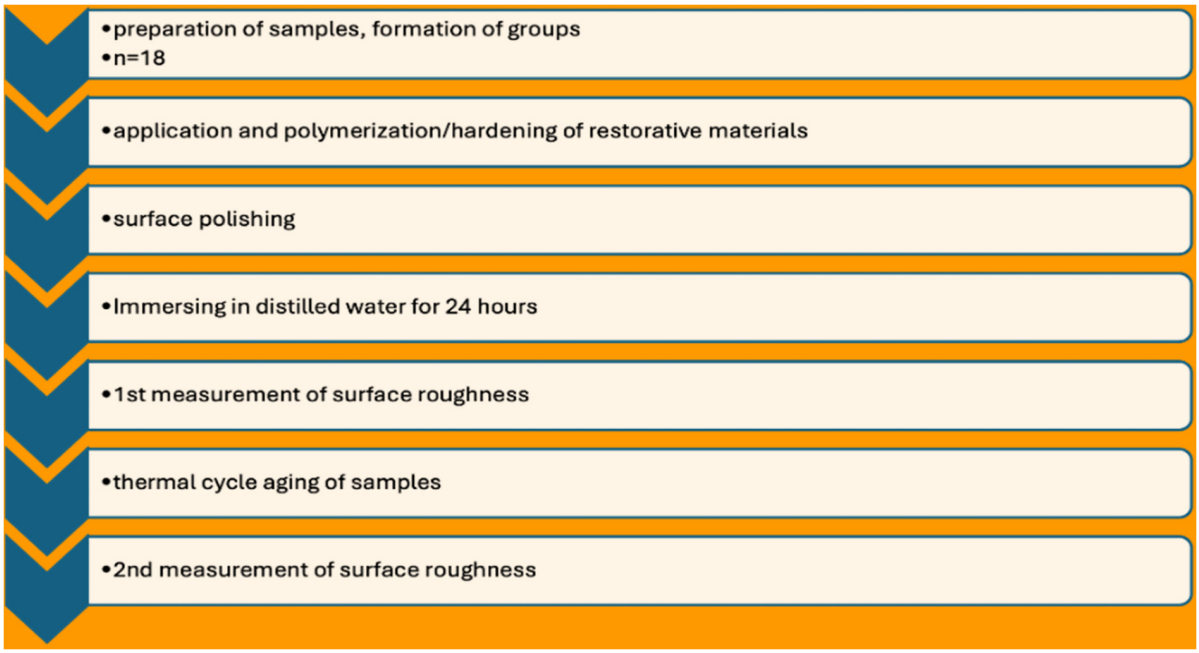


Figure 2. Schematic illustration of the Class V cavity preparation and the methodology of sample preparation and surface roughness measurements.

Group 1: EQUIA Forte (EF) and Group 4: Fuji II Light Cure (F)

The prepared cavities were dried using an air/water spray. EQUIA Forte and Fuji II LC capsules were mixed in a capsule mixer (ZoneRay, Treedental, Hangzhou, China) for 10 s and inserted into the cavities in bulk using a gun extractor. The materials were adapted to the cavity margins with a spatula according to the manufacturers' instructions. Fuji II LC specimens were additionally light cured for 20 s using an LED curing unit (VALO Cordless,

Ultradent Inc., South Jordan, UT, USA; output intensity: 1200 mW/cm^2). Light output was verified using a Demetron LED radiometer (Kerr, Middleton, WI, USA) [47]. EQUIA Forte specimens were coated with a resin-based surface coating (EQUIA Forte Coat, GC, Tokyo, Japan) and polymerized for 20 s.

Group 2: Cention-N (CN), Group 3: Activa BioActive Restorative (AB), and Group 5: Solare-X (SX)

The cavities were dried using an air/water spray. Enamel and dentin were etched for 30 s and 15 s, respectively, using 37% orthophosphoric acid, followed by a 30 s rinse and gentle air-drying. A universal adhesive system (Clearfil Tri-S Bond Universal, Kuraray, Japan) was applied using agitation, and the solvent was evaporated with a mild air stream for 5 s. The adhesive layer was polymerized for 10 s using the same LED curing unit. The restorative materials were placed according to the manufacturers' instructions.

All restorations were finished and polished using polishing discs (Optidisc, Kerr, Middleton, WI, USA) under water cooling. Subsequently, all specimens were stored in distilled water at room temperature for 24 h to allow post-polymerization [48].

2.2. Areal Surface Roughness Measurement (Sa)

The initial surface roughness of the samples was assessed using a non-contact profilometer (Polytech TMS100/100 TopMap, Munich, Germany) at the Mechanical Engineering Department of Gaziantep University, following a 24-h immersion in distilled water at room temperature.

Ninety specimens made of five different dental materials (n = 18/group) were subjected to surface roughness measurements. The initial surface roughness of the samples was assessed using a non-contact profilometer (Polytech TMS100/100 TopMap, Munich, Germany) at the Mechanical Engineering Department of Gaziantep University, following a 24-h immersion in distilled water. (Turkey; MOS LAB, Ankara, Turkey).

Prior to surface roughness measurement processes, the correlogram obtained by coherence scanning (Figure 3a) was subjected to a series of filtering processes since the raw data obtained by scanning contains noise, surface form, waviness, and roughness. The aim was to eliminate noise and surface form and focus on the roughness of the restorations. The procedure specified in the ISO 25178-2 standard [49] was followed for the filtering processes. First, an 8 µm Gaussian low-pass filter was used to construct the primary surface and filter out noise. Subsequently, a second-order polynomial form operation was performed on both axes for the form removal process on the primary surface. A higher-order polynomial fit was avoided in order not to suppress surface roughness. Finally, a Gaussian high-pass filter with a wavelength of 2500 µm was used to separate surface waviness from roughness. In order not to affect the surface roughness values, no averaging or median filtering was applied, even to increase the measured pixels. The improved surface topography obtained because of the aforementioned filter sequence is shown in Figure 3b.

To determine Sa, three different areas were determined on the filtered surface, namely Cement/Material interface, Enamel/Material interface, and Material Surface. For the measurements not to be affected by the differentiation of area, the maximum reproducible measurement fields of 400 × 1600 µm^2, 1600 × 400 µm^2, and 800 × 800 µm^2 were determined for Cement/Material interface, Enamel/Material interface, and Material Surface respectively. All samples, respectively, cover the same area in all three sections. The measurement fields are shown in Figure 4a. A cut-off wavelength of 2500 µm was used for all samples. To measure the same position of the surface on all samples, a recipe was created, and all samples were measured using the same recipe. As seen in Figure 4b, although the dental filling is a free-form surface, high pixel measurements were provided within the

determined fields. The measurable part within the determined areas for all samples is over 95%.

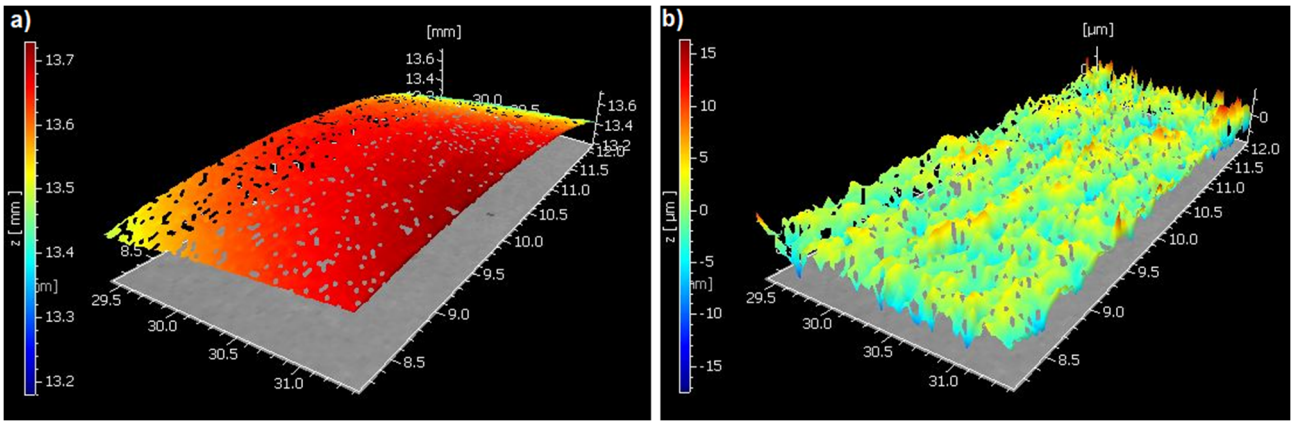


Figure 3. (**a**) Coherence scanned raw data of surface topography. (**b**) The improved topography by filter sequence.

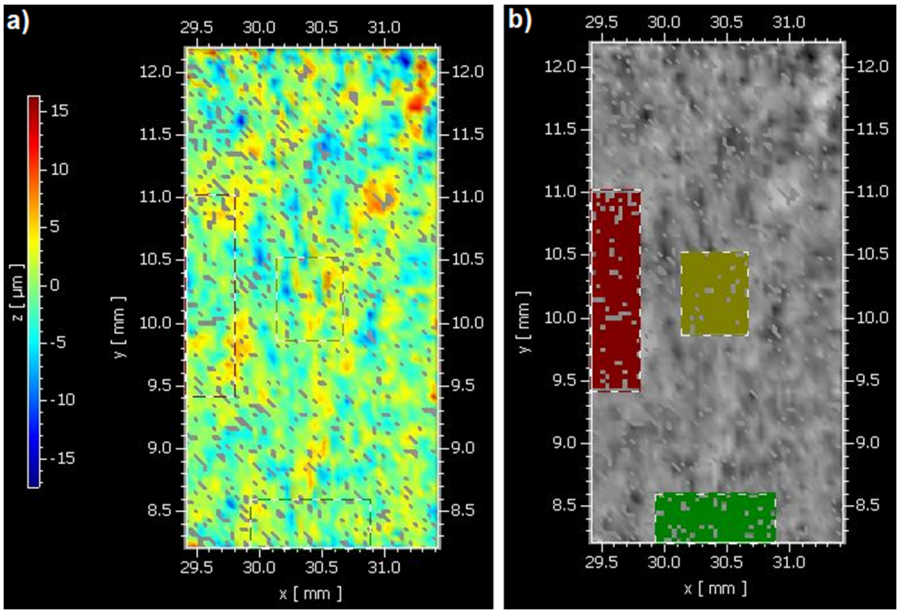


Figure 4. (**a**) Sa measurement fields of cement/material interface, enamel/material interface, and material surfaces. (**b**) The measured pixels in cement/material (red dotted rectangular area), enamel/material (bright green dotted rectangular area), and material surfaces (khaki green dotted rectangular area).

After the surface roughness measurement, to simulate the intraoral environment, thermal cycles were applied with a Thermocycler (SD mechatronic, Munich, Germany) for 10,000 times between 5 and 55 °C of water with a bath duration of 50 s and a transition time of 10 s between them [40]. After the aging process, the surface roughness measurements of the samples were repeated, and the final measurement values were recorded in Sa (µm).

2.3. Statistical Analysis

All statistical analyses were performed using SPSS software (version 24.0; SPSS Inc., Chicago, IL, USA). The normality of data distribution was assessed with the Shapiro–Wilk test. Since the assumptions for parametric testing were met, two-way repeated measures ANOVA was applied to evaluate the effects of material type, surface region (cement/material interface, enamel/material interface, and material surface), and thermo-

cycling (before and after aging) on surface roughness values (Sa). Interaction effects among these factors were also examined. When significant main or interaction effects were detected, Tukey's HSD test was performed for post hoc pairwise comparisons. Mauchly's test of sphericity was used to check the assumption of sphericity, and Greenhouse–Geisser correction was applied when necessary. Statistical significance was set at $p < 0.05$ (two-tailed).

3. Results

Table 2 and Figure 5 display the outcomes of the samples' surface roughness analysis. It was determined that the material and surface types had a statistically significant effect on the change in initial and final roughness with different surface types and groups ($p < 0.05$).

Table 2. Comparison of initial and after-aging (final) roughness values (Sa; µm) for different groups, solutions, and surface types.

	Cement/Material Interface		Enamel/Material Interface		Material Surface	
	Initial Mean (sd)	Final Mean (sd)	Initial Mean (sd)	Final Mean (sd)	Initial Mean (sd)	Final Mean (sd)
Activa BioActive Restorative (AB)	3.87 (1.61) ^{Ab}	5.92 (2.29) ^{Aa}	3.69 (1.58) ^{Abc}	5.09 (1.98) ^{Bb}	1.36 (0.52) ^{Aa}	1.74 (0.89) ^{Ba}
Cention-N (CN)	4.08 (1.99) ^{Aab}	6.15 (2.38) ^{Bbc}	4.17 (1.53) ^{Ac}	6.12 (2.47) ^{Bb}	2.98 (1.79) ^{Ab}	3.6 (1.78) ^{Bb}
Equia Forte (EF)	5.07 (2) ^{Ac}	7.45 (2.05) ^{Bc}	3.97 (2.04) ^{Ac}	6.04 (1.97) ^{Bb}	3.26 (1.81) ^{Ab}	4.09 (2.07) ^{Bb}
Fuji II LC (F)	3.11 (1.69) ^{Ab}	4.34 (2.56) ^{Bab}	2.95 (0.64) ^{Ab}	3.81 (0.92) ^{Ba}	1.47 (0.61) ^{Aa}	1.84 (0.67) ^{Ba}
Solare-X (SX)	1.96 (1.13) ^{Aa}	3.68 (1.98) ^{Ba}	1.71 (0.91) ^{Aa}	2.63 (1.61) ^{Ba}	0.83 (0.29) ^{Aa}	1.02 (0.42) ^{Ba}

The means that are significantly different ($p < 0.05$) are shown by distinct capital letters in the same row and lowercase letters in the same column.

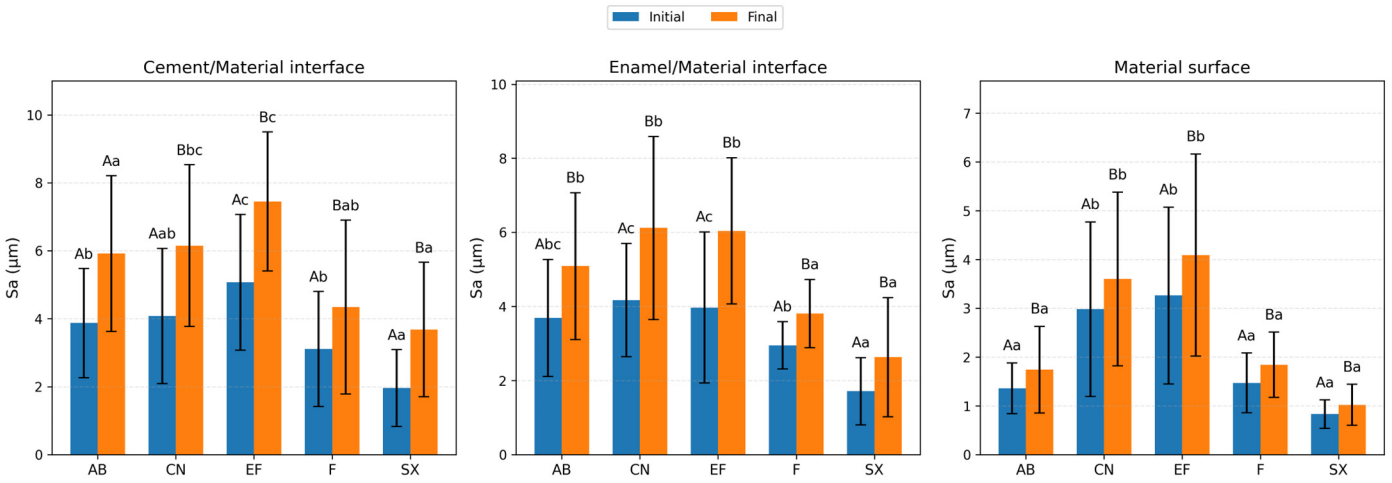


Figure 5. Comparison of initial and after-aging (final) roughness values. The same letters on the bars indicate that there are no difference between the groups.

When the initial and final surface roughness measurements were analyzed, the SX group showed less roughness compared to the others ($p = 0.001$). Following this group, the F and AB groups showed significantly less roughness compared to the CN and EF groups ($p < 0.05$). No significant difference was detected between the F-AB and CN-EF groups.

In the combined analysis of all material groups, the roughness values at the cement/material and enamel/material interfaces were not statistically different ($p = 0.065$). Nevertheless, both interfaces demonstrated significantly higher roughness compared to the material surfaces across all groups ($p < 0.05$). Exact p-values for before–after comparisons of each material and surface type are presented in Table 3.

Table 3. Exact *p*-values were obtained from Tukey's HSD post hoc test following two-way repeated measures ANOVA of the different interfaces and surface.

Material	Cement/Material Interface	Enamel/Material Interface	Material Surface
Activa BioActive Restorative	<0.001	<0.001	0.010
Cention-N	<0.001	<0.001	<0.001
Equia Forte	<0.001	<0.001	0.018
Fuji II LC	<0.001	<0.001	<0.001
Solare-X	<0.001	<0.001	0.007

4. Discussion

This study investigated the in vitro effect of thermal cycle aging, simulating one year of intraoral use, on the roughness of the material/enamel interfaces, material/cement interfaces, and material surfaces. The study's null hypotheses were all rejected because thermal cycles affected negatively the surface roughness on different tooth surfaces.

Teeth in the oral cavity are continuously subject to stresses due to chewing forces, saliva, physical and chemical factors from food and beverages with various pH levels [50]. Therefore, one of the most often used artificial aging approaches is the thermal cycle aging, which imitates the circumstances of the oral environment in vitro. In many in vitro studies, distilled water was preferred as the storage solution of the samples [51]. Therefore, it was the preferred solution used in our study as well.

Surface roughness may adversely affect the marginal integrity of restorative materials, leading to an increased risk of gingival inflammation. In addition, rough restoration surfaces can cause discoloration and plaque accumulation. Previous studies have indicated that surface roughness values above 0.2 μm may already increase bacterial adhesion and plaque retention [52]. Profilometer devices can measure the surface structure of the materials in two dimensions and are used to measure areal surface roughness. Roughness values obtained by profilometers contain the results of quantitative measurement of surface irregularities [53]. In many studies, stylus-type roughness measuring devices have been employed to assess the surface roughness of dental materials [25,48,54]. In this study, instead of the stylus-type line profile measurement method, which has limited performance in describing the complete topography [55], Coherence Scanning White Light Interferometry [56] (WLI) (Polytec TMS-100 TopMap Metro. Lab, Waldbronn, Germany) has been used for the measurement of bio-interactive material's surfaces. Thus, areal roughness measurements, not limited to only linear profiles, have been performed on the dental material surface. Often, the areal arithmetic average roughness Sa is used to define the true surface texture. Sa is related to the measurement field (A) of the topography and can be calculated by the below equation using a quadratic integral [57].

$$Sa = \frac{1}{A}\iint |z(x,y)|dxdy \quad (1)$$

Several in vitro investigations that examined the surface roughness of various restorative materials used silicone, polyethylene, metal, and other molds to create the specimens [58]. This technique solely allows for the evaluation of the material's surface roughness. However, the objective of this study was to evaluate the surface roughness of the material/enamel and material/cement interface in addition to the material's surface. Therefore, the specimens in this study were prepared and restored with Class V cavities performed in extracted impacted third molar teeth.

Marginal gaps resulting from inadequate marginal adaptation not only increase the risk of secondary caries at the restoration margins but also negatively affect surface smoothness, thereby compromising the esthetic outcome and clinical durability of the restoration [59,60]. Therefore, achieving both proper marginal adaptation and a smooth surface through appropriate finishing and polishing procedures is crucial for the long-term success of restorative treatments [60]. The study's findings indicate that a greater increase in surface roughness at the material/enamel and material/cementum interfaces after thermal aging was observed compared to the material surface. This result may be due to microleakage that may have occurred between the tooth tissue/restoration interfaces [50,61]. The surface roughness of the restorative material is directly relevant to the material structure. Filler type, composition, chemistry, quantity, and size all affect the material's surface roughness. Composite resin materials should have a smooth surface after finishing/polishing and should sustain these surface properties for a long time under various physical and chemical conditions in the oral environment [62].

Glass ionomer cements (GICs), which chemically bond to tooth structure and have anti-caries capabilities by enabling the release of fluoride, have been developed as an alternative to amalgam and composite resin materials, which are frequently used due to their high aesthetic and physical features. However, glass ionomer cements exhibit lower mechanical, physical, and aesthetic properties compared to composite resins. All these problems have been minimized by the materials evolution with the improvements in glass ionomer technologies (resin-modified glass ionomers, high-viscosity glass ionomers, bio-interactive materials, etc.). Additionally, dentists have lately started to use dual-cure bulk-fill composite resins, which are notable for their simplicity of handling and may be applied in the cavity as a single increment [61,63]. Dual-cure bulk-fill composite resins provide effective polymerization in areas where light cannot reach, claiming to eliminate the problems associated with insufficient light-curing [64,65]. In this study, a high-viscosity glass ionomer (Equia Forte), a resin-modified glass ionomer cement (Fuji II LC), a bio-interactive material (Activa BioActive Restorative), and a dual-cure bulk-fill alcasite restorative material (Cention-N) were used. In addition, Solare-X, a conventional nanofilled composite resin, was used as a control group.

Surface roughness is one of the most crucial variables in defining the surface properties of restorative materials. Therefore, it is frequently used to ascertain the surface properties of restorative materials. Undesirable results, such as high surface roughness, reduce the quality of the restoration and its longevity. As a result, high surface roughness can negatively impact the material's mechanical and physical qualities and increase the restoration's water absorption [66]. Considering all these reasons, the effect of thermal cycles aging on different bio-interactive restorative materials was compared. Compared to the other groups, the nanofilled composite Solare-X showed significantly lower surface roughness. This may be explained by the small size of the inorganic filler particles in the substance, which, after finishing and polishing, allows for smoother surfaces [67].

When comparing the surface roughness of AB and EF groups stored in distilled water for 24 h prior to thermal cycling, Kazak et al. [50] reported no statistically significant differences between the two materials at baseline. Moreover, they also found that even after thermal aging, the surface roughness values of AB and EF remained statistically comparable, indicating that both materials showed a similar response to the aging process. In the study conducted by Güner and Köse [68] which evaluated the surface roughness of fluoride-releasing dental materials immersed in distilled water for 24 h, it was observed that EF samples exhibited rougher surfaces than AB samples. Similarly, the AB group in this study exhibited less roughness than the EF group in both initial and post-thermal cycle tests. This result is probably related to the formulation of the material including urethane

dimethacrylate, instead of bisphenol A glycidyl methacrylate [69]. In the study by Atalay and Yazıcı [17] evaluating the effect of radiotherapy on the surface roughness of various bio-active restorative materials, when the pre-radiotherapy (initial) measurements were examined, the surface roughness of EF, AB, and CN samples did not show any statistical differences. However, in the study's initial material surface roughness measurements, the CN and EF group samples displayed higher surface roughness than the AB group. This could be explained by the CN group samples' non-homogeneous structure because of the powder-liquid form's manual mixing. Out of all the restorative materials that were examined, EF had the highest surface roughness when it endured thermal cycles of aging. This outcome could be attributed to the glass ionomer-based materials' internal porous nature or to the potentially bubble-filled mixing and application processes. The use of nanoparticle resin-based coatings to increase the surface smoothness and wear resistance of glass ionomer and glass hybrid restorative materials is an effective application supported by clinical and laboratory studies [70,71]. An in vitro study conducted by Kanik et al. [72] underlined this protective effect with the statement "resin coating protects the glass ionomer materials from excessive wear until 20,000 cycles" and showed that, if it provides protection, it brings the material to a similar wear level as resin composites. Following the manufacturer's instructions, a resin-based coating was applied to the surface of the EF group samples during sample preparation. This coating fills the surface micropores, smoothest the topography and thus creates a physical barrier that limits moisture penetration, contributing to the preservation of the surface integrity of the material during the early maturation process. This approach helps to maintain the structural stability of the material by reducing its susceptibility to both excessive water absorption and water loss [71]. This protective layer minimizes microcrack formation and surface erosion by abrasive forces by increasing flexural and chemical resistance. As a result, surface roughness decreases significantly in coated materials, while flexural and pressurized strength increases. In the study conducted by Ugurlu, after one year of water aging, the roughness values of coated glass ionomer samples were significantly lower compared to uncoated groups [73].

There is currently no universally accepted clinical threshold for surface roughness (Ra) in the literature. Some studies have suggested that Ra values between 0.7 and 1.4 μm do not result in significant changes in plaque accumulation [74], whereas Bollen et al. [75] reported that Ra values exceeding 0.2 μm are associated with increased plaque retention. Furthermore, when Ra values exceed 0.5 μm, surface roughness may become perceptible to patients [76]. In the present study, the evaluation was performed using the arithmetic mean surface area parameter (Sa). Since previous findings in the literature are primarily reported in terms of Ra, direct comparison with the present results is not possible. To the best of our knowledge, this is the first study in dentistry to assess surface changes of bio-interactive restorative materials using the Sa parameter.

Optical profilometry was preferred in this study for its precise evaluation of surface morphology, and some other advantages compared to the classical stylus profilometry that have been emphasized in the literature earlier [77,78]. Optical profilometers (interferometry, confocal, etc.) work without contact with the surface and therefore prevent surface deformation in materials [79]. The results are obtained with high resolution, and the entire surface microstructure is recorded which is impossible with the classic stylus profilometer method. Moreover, the optical method provides a 3D (areal) surface topography and can scan larger areas, whereas stylus profilometry evaluates only a single 2D slice and may miss local surface irregularities. Optical systems can record millions of data points in seconds, and the device calibration requires less maintenance. On the contrary, stylus devices have moving parts and can be affected by ambient noise [31,75]. Although optical profilometers can be affected by features such as surface curvature, high roughness

or optical reflection [31], in our study, to overcome these problems, the raw correlogram data obtained by coherence scanning interferometry after measurement was subjected to a filtering process in accordance with the ISO 25178-2 standard [49]. With these processes, surface form, waviness and noise were removed; and the focus was only on roughness. Thus, the limitations of optical systems were minimized, and the surface properties of restorative materials could be analyzed reliably and accurately.

The increased surface roughness observed at the enamel/material and cement/material interfaces after thermal aging may be related to changes in interfacial bonding mechanisms over time. Previous studies have demonstrated that the stability of material–tooth connections is influenced by factors such as hydrolytic degradation, thermal stress, and differences in the coefficients of thermal expansion between restorative materials and dental tissues. Degradation of adhesive interfaces and ion-mediated interactions may contribute to interfacial roughening under aging conditions, which is consistent with the principles of material connections described in the literature. These findings align with previous reports highlighting time-dependent changes in adhesive and restorative interfaces under simulated oral conditions [80,81].

This in vitro study has certain limitations that should be considered when interpreting the findings. Surface characterization was limited to areal surface roughness (Sa) assessed by non-contact profilometry; therefore, other clinically relevant parameters such as microleakage, marginal integrity, mechanical loading, toothbrushing simulation, erosive challenges, and detailed morphological or chemical analyses (e.g., SEM) were not evaluated. In addition, the use of extracted human teeth under laboratory conditions cannot fully reproduce the complex oral environment, including saliva dynamics, pH fluctuations, biofilm activity, and masticatory forces. Only a single finishing and polishing protocol was applied, although different clinical protocols may result in variations in surface characteristics. Furthermore, the relatively limited sample size and the inclusion of a single composite resin as a control may restrict the generalizability of the results. Future studies incorporating larger sample sizes, extended aging protocols, mechanical loading, and complementary surface and interfacial analyses are warranted to provide a more comprehensive assessment of bio-interactive restorative materials.

5. Conclusions

Within the limitations of this in vitro study, thermal aging significantly increased the surface roughness of all tested restorative materials. Among the evaluated materials, Solare-X consistently exhibited the lowest roughness values both before and after aging, whereas Cention-N and Equia Forte demonstrated comparatively higher roughness values. In addition, surface roughness at the enamel/material and cement/material interfaces was significantly greater than that measured on the material surfaces themselves. The increased roughness observed at the interfacial regions suggests a higher susceptibility to plaque retention and interfacial degradation, which may adversely affect the long-term clinical performance of restorations. Future studies incorporating long-term aging protocols, mechanical loading, and complementary surface characterization methods may further clarify the clinical relevance of interfacial roughness changes observed in bio-interactive restorative materials.

Author Contributions: Conceptualization, Z.G.; methodology, Z.G.; validation, Z.G., G.K. and S.O.; formal analysis, Z.G., G.K., S.O. and H.Ç.; investigation, Z.G., G.K., S.O., H.Ç. and A.G.B.; resources, Z.G.; data curation, Z.G., G.K., S.O. and H.Ç.; writing—original draft preparation, Z.G., G.K., S.O. and L.S.T.; writing—review and editing, all authors; visualization, Z.G.; supervision, Z.G.; project administration. All authors have read and agreed to the published version of the manuscript.

Funding: This research received no external funding.

Institutional Review Board Statement: This study was conducted in full accordance with the principles of the Declaration of Helsinki and was approved by the Non-Interventional Clinical Research Ethics Committee of Gaziantep University (Approval No: 2024/325). Written informed consent was voluntarily obtained from all participants or their legal guardians.

Data Availability Statement: All essential data is presented in the manuscript. The datasets used and/or analyzed during the current study are available from the corresponding author on reasonable request.

Conflicts of Interest: No conflicts of interest were declared among the authors.

Abbreviations

AB	Activa BioActive Restorative
CN	Cention-N
EF	Equia Forte
F	Fuji II Light-cured
GIC	Glass ionomer cement
ISO	International Organization for Standardization
LED	Light-emitting diode
SX	Solare-X
µm	micrometer

References

1. Doğu Kaya, B.; Acar, E.; Farshidian, N.; Göçmen, G.B.; Tarçın, B.; Atalı, P.Y.; Tarçın, B. The effect of cavity disinfectant on microleakage of self adhesive composite restorations in class V cavities. *Eur. J. Res. Dent.* **2023**, *7*, 115–121. [CrossRef]
2. Lokhande, N.A.; Padmai, A.S.; Rathore, V.P.S.; Shingane, S.; Jayashankar, D.N.; Sharma, U. Effectiveness of flowable resin composite in reducing microleakage—An in vitro study. *J. Int. Oral Health* **2014**, *6*, 111–114. [PubMed]
3. Alcaraz, M.G.R.; Veitz Keenan, A.; Sahrmann, P.; Schmidlin, P.R.; Davis, D.; Iheozor Ejiofor, Z. Direct composite resin fillings versus amalgam fillings for permanent or adult posterior teeth. *Cochrane Database Syst. Rev.* **2014**, CD005620. [CrossRef]
4. Favetti, M.; Montagner, A.F.; Fontes, S.T.; Martins, T.M.; Masotti, A.S.; Jardim, P.D.S.; Corrêa, F.O.B.; Cenci, M.S.; Muniz, F.W.M.G. Effects of cervical restorations on periodontal tissues: 5 year follow up of a randomized clinical trial. *J. Dent.* **2021**, *106*, 103571. [CrossRef]
5. Slimani, A.; Sauro, S.; Gatón Hernández, P.; Gurgan, S.; Turkun, L.S.; Miletic, I.; Banerjee, A.; Tassery, H. Commercially available ion releasing dental materials and cavitated carious lesions: Clinical treatment options. *Materials* **2021**, *14*, 6272. [CrossRef] [PubMed]
6. Nedeljkovic IDe Munck, J.; Slomka, V.; Van Meerbeek, B.; Teughels, W.; Van Landuyt, K.L. Lack of buffering by composites promotes shift to more cariogenic bacteria. *J. Dent. Res.* **2016**, *95*, 875–881. [CrossRef]
7. Hench, L.L. Bioceramics: From concept to clinic. *J. Am. Ceram. Soc.* **1991**, *74*, 1487–1510. [CrossRef]
8. Hench, L.L.; Polak, J.M. Third generation biomedical materials. *Science* **2002**, *295*, 1014–1017. [CrossRef]
9. Kokubo, T.; Kim, H.M.; Kawashita, M. Novel bioactive materials with different mechanical properties. *Biomaterials* **2003**, *24*, 2161–2175. [CrossRef]
10. Kim, H.G.; Lee, B.N.; Jeong, H.J.; Kim, H.J.; Kwon, J.; Oh, S.; Kim, D.-S.; Choi, K.-K.; Kim, R.H.; Jang, J.-H. Effect of bioactive glass into mineral trioxide aggregate on biocompatibility and mineralization potential of dental pulp stem cells. *Biomater. Res.* **2025**, *29*, 0142. [CrossRef]
11. Hiremath, G.; Pramanik, S.; Horatti, P. Comparative evaluation of bioactivity of MTA Plus and MTA Plus chitosan conjugate in phosphate buffer saline: An in vitro study. *Saudi Dent. J.* **2024**, *36*, 1097–1104. [CrossRef]
12. Primus, C.; Gutmann, J.L.; Tay, F.R.; Fuks, A.B. Calcium silicate and calcium aluminate cements for dentistry reviewed. *J. Am. Ceram. Soc.* **2022**, *105*, 1841–1863. [CrossRef]
13. Gündoğar, Z.U.; Keskin, G.; Yaman Küçükersen, M. Shear Bond Strength of Biointeractive Restorative Materials to NeoMTA Plus and Biodentine. *Polymers* **2025**, *17*, 3070. [CrossRef] [PubMed]
14. Pires, P.M.; Neves, A.D.A.; Makeeva, I.M.; Schwendicke, F.; Faus-Matoses, V.; Yoshihara, K.; Banerjee, A.; Sauro, S. Contemporary restorative ion-releasing materials: Current status, interfacial properties and operative approaches. *Br. Dent. J.* **2020**, *229*, 450–458. [CrossRef]

15. Schmalz, G.; Hickel, R.; Price, R.B.; Platt, J.A. Bioactivity of dental restorative materials: FDI policy statement. *Int. Dent. J.* **2023**, *73*, 21–27. [CrossRef]
16. Almuhaiza, M. Glass-ionomer cements in restorative dentistry: A critical appraisal. *J. Contemp. Dent. Pract.* **2016**, *17*, 331–336. [CrossRef] [PubMed]
17. Atalay, C.; Yazici, A.R. Effect of radiotherapy on surface roughness and microhardness of contemporary bioactive restorative materials. *Support. Care Cancer* **2024**, *32*, 295. [CrossRef]
18. Singh, S.; Kulkarni, G.; Kumar, R.S.M.; Jain, R.; Lokhande, A.M.; Sitlaney, T.K.; Ansari, M.H.F.; Agarwal, N.S. Comparative evaluation of biological response of conventional and resin-modified glass ionomer cement on human cells: A systematic review. *Restor. Dent. Endod.* **2024**, *49*, e41. [CrossRef]
19. GC Fuji II LC Capsule—Instructions for Use. Available online: https://gclatinamerica.com/assets/doctos/descargas/111/F2LCbrochure.pdf (accessed on 25 December 2025).
20. Ruengrungsom, C.; Burrow, M.F.; Parashos, P.; Palamara, J.E.A. Evaluation of F, Ca, and P release and microhardness of eleven ion-leaching restorative materials and recharge efficacy using new Ca/P fluoride varnish. *J. Dent.* **2020**, *102*, 103474. [CrossRef]
21. Theerarath, T.; Sriarj, W. An alkasite restorative material effectively remineralized artificial interproximal enamel caries in vitro. *Clin. Oral Investig.* **2022**, *26*, 4437–4445. [CrossRef] [PubMed]
22. Garoushi, S.; Vallittu, P.K.; Lassila, L. Characterization of fluoride releasing restorative dental materials. *Dent. Mater. J.* **2018**, *37*, 293–300. [CrossRef]
23. Jaramillo-Cartagena, R.; López-Galeano, E.J.; Latorre-Correa, F.; Agudelo-Suárez, A.A. Effect of polishing systems on the surface roughness of nano-hybrid and nano-filling composite resins: A systematic review. *Dent. J.* **2021**, *9*, 95. [CrossRef] [PubMed]
24. Hao, Y.; Huang, X.; Zhou, X.; Li, M.; Ren, B.; Peng, X.; Cheng, L. Influence of dental prosthesis and restorative materials interface on oral biofilms. *Int. J. Mol. Sci.* **2018**, *19*, 3157. [CrossRef] [PubMed]
25. Babina, K.; Polyakova, M.; Sokhova, I.; Doroshina, V.; Arakelyan, M.; Novozhilova, N. The effect of finishing and polishing sequences on the surface roughness of three different nanocomposites and composite/enamel and composite/cementum ınterfaces. *Nanomaterials* **2020**, *10*, 1339. [CrossRef]
26. Ereifej, N.S.; Oweis, Y.G.; Eliades, G. The effect of polishing technique on 3-D surface roughness and gloss of dental restorative resin composites. *Oper. Dent.* **2013**, *38*, E1–E12. [CrossRef]
27. Chour, R.G.; Moda, A.; Arora, A.; Arafath, M.Y.; Shetty, V.K.; Rishal, Y. Comparative evaluation of effect of different polishing systems on surface roughness of composite resin: An in vitro study. *J. Int. Soc. Prev. Community Dent.* **2016**, *6*, 166–170. [CrossRef]
28. Chiang, Y.C.; Lai, E.H.H.; Kunzelmann, K.H. Polishing mechanism of light-initiated dental composite: Geometric optics approach. *J. Formos. Med. Assoc.* **2016**, *115*, 1053–1060. [CrossRef]
29. Kakaboura, A.; Fragouli, M.; Rahiotis, C.; Silikas, N. Evaluation of surface characteristics of dental composites using profilometry, scanning electron, atomic force microscopy and gloss-meter. *J. Mater. Sci. Mater. Med.* **2007**, *18*, 155–163. [CrossRef]
30. Rosentritt, M.; Schneider-Feyrer, S.; Kurzendorfer, L. Comparison of surface roughness parameters R_a/S_a and R_z/S_z with different measuring devices. *J. Mech. Behav. Biomed. Mater.* **2024**, *150*, 106349. [CrossRef] [PubMed]
31. Leach, R.; Haitjema, H. Bandwidth characteristics and comparisons of surface texture measuring instruments. *Meas. Sci. Technol.* **2010**, *21*, 079801. [CrossRef]
32. Vorburger, T.V.; Rhee, H.-G.; Renegar, T.B.; Song, J.-F.; Zheng, A. Comparison of optical and stylus methods for measurement of surface texture. *Int. J. Adv. Manuf. Technol.* **2007**, *33*, 110–118. [CrossRef]
33. Holthuizen, P.; Çopuroğlu, O. Quantification of surface grinding during the sample preparation of cementitious materials by optical profilometry. *J. Microsc.* **2024**, *294*, 128–136. [CrossRef]
34. Demircioglu, P. A comparison between contact type profilometer and different 3D optical techniques: A case study in characterization of machined surface structures. In Proceedings of the 2nd International Conference on Quality and Innovation in Engineering and Management, Cluj-Napoca, Romania, 22 November 2012; pp. 117–122.
35. *EN ISO 25178-1:2016*; Geometrical Product Specifications (GPS)—Surface Texture: Areal-Part 1, Indication of Surface Texture. International Organization for Standardization: Geneva, Switzerland, 2016.
36. Park, J.-B.; Jeon, Y.; Ko, Y. Effects of titanium brush on machined and sand-blasted/acid-etched titanium disc using confocal microscopy and contact profilometry. *Clin. Oral Implants Res.* **2015**, *26*, 130–136. [CrossRef]
37. Bodnar, D.; Dumitriu, A.; Suciu, I.; Dimitriu, B.; Chirilă, M.; Bartok, R.; Ciocârdel, M.; Țâncu, A.M.; Straja, D. Microscopic and statistical evaluation of the marginal defects of composite restorations: In vitro studies. *J. Med. Life* **2024**, *17*, 625–633. [CrossRef]
38. Yadav, G.; Rehani, U.; Rana, V. A Comparative Evaluation of Marginal Leakage of Different Restorative Materials in Deciduous Molars: An in Vitro Study. *Int. J. Clin. Pediatr. Dent.* **2012**, *5*, 101–107. [CrossRef] [PubMed]
39. Tuncer, S.; Demirci, M.; Tiryaki, M.; Ünlü, N.; Uysal, Ö. The effect of a modeling resin and thermocycling on the surface hardness, roughness, and color of different resin composites. *J. Esthet. Restor. Dent.* **2013**, *25*, 404–419. [CrossRef] [PubMed]
40. Scholz, K.J.; Hinderberger, M.; Widbiller, M.; Federlin, M.; Hiller, K.; Buchalla, W. Influence of Selective Caries Excavation on Marginal Penetration of Class II Composite Restorations in Vitro. *Eur. J. Oral Sci.* **2020**, *128*, 405–414. [CrossRef]

41. Ferreira, M.C.; Vieira, R.S. Marginal leakage in direct and ındirect composite resin restorations in primary teeth: An in vitro study. *J. Dent.* **2008**, *36*, 322–325. [CrossRef]
42. Cenci, M.S.; Pereira-Cenci, T.; Donassollo, T.A.; Sommer, L.; Strapasson, A.; Demarco, F.F. Influence of thermal stress on marginal integrity of restorative materials. *J. Appl. Oral Sci.* **2008**, *16*, 106–110. [CrossRef]
43. Boussès, Y.; Brulat-Bouchard, N.; Bouchard, P.O.; Tillier, Y. A numerical, theoretical and experimental study of the effect of thermocycling on the matrix-filler interface of dental restorative materials. *Dent. Mater.* **2021**, *37*, 772–782. [CrossRef] [PubMed]
44. Kim, S.H.; Choi, Y.S.; Kang, K.H.; Att, W. Effects of thermal and mechanical cycling on the mechanical strength and surface properties of dental cad-cam restorative materials. *J. Prosthet. Dent.* **2022**, *128*, 79–88. [CrossRef]
45. Salerno, M.; Loria, P.; Matarazzo, G.; Tomè, F.; Diaspro, A.; Eggenhöffner, R. Surface morphology and tooth adhesion of a novel nanostructured dental restorative composite. *Materials* **2016**, *9*, 203. [CrossRef]
46. Cohen, J. *Statistical Power Analysis for the Behavioral Sciences*, 2nd ed.; Lawrence Erlbaum Associates: Hillsdale, NJ, USA, 1988.
47. Furuse, A.Y.; Santana, L.O.C.; Rizzante, F.A.P.; Ishikiriama, S.K.; Bombonatti, J.F.; Correr, G.M.; Gonzaga, C.C. Delayed light activation improves color stability of dual-cured resin cements. *J. Prosthodont.* **2018**, *27*, 449–455. [CrossRef]
48. Kose, H.D.; Giray, I.; Boyacioglu, H.; Turkun, L.S. Can energy drinks affect the surface quality of bioactive restorative materials? *BMC Oral Health* **2024**, *24*, 1011. [CrossRef]
49. *EN ISO 25178-2:2022*; Geometrical Product Specifications (GPS)—Surface texture: Areal-Part 2, Terms, Definitions and Surface Texture Parameters. International Organization for Standardization: Geneva, Switzerland, 2022.
50. Kazak, M.; Koymen, S.; Yurdan, R.; Tekdemir, K.; Donmez, N. Effect of thermal aging procedure on the microhardness and surface roughness of fluoride ion containing materials. *Ann. Med. Res.* **2020**, *27*, 888. [CrossRef]
51. Do Amaral, F.L.; Colucci, V.; De Souza-Gabriel, A.E. Adhesion to er: Yag laser-prepared dentin after long- term water storage and thermocycling. *Oper. Dent.* **2008**, *33*, 51–58. [CrossRef]
52. Alshali, R.Z.; Silikas, N.; Satterthwaite, J.D. Surface roughness evaluation of resin composites after prolonged aging and different polishing protocols. *Int. J. Dent.* **2023**, *2023*, 4078788.
53. Bakar, W.; Mcintyre, W.Z. Susceptibility of selected tooth-coloured dental materials to damage by common erosive acids. *Aust. Dent. J.* **2008**, *53*, 226–234. [CrossRef] [PubMed]
54. Niazi, F.H.; Alotaibi, B.; Abdulla, A.M.; AlTowayan, S.A.; Ahmed, S.Z.; Alshehri, D.; Samran, A.; Alsuwayyigh, N.; Luddin, N. Modified experimental adhesive with sepiolite nanoparticles on caries dentin treated with femtosecond laser and photodynamic activated erythrosine. An in vitro study. *Photodiagn. Photodyn. Ther.* **2024**, *49*, 104306. [CrossRef] [PubMed]
55. *EN ISO 25178-6:2010*; Geometrical Product Specifications (GPS)—Surface texture: Areal-Part 6: Classification of Methods for Measuring Surface Texture. International Organization for Standardization: Geneva, Switzerland, 2010.
56. *EN ISO 25178-604:2013*; Geometrical Product Specifications (GPS)—Surface texture: Areal-Part 604: Nominal Characteristics of Non-Contact (Coherence Scanning Interferometry) Instruments. International Organization for Standardization: Geneva, Switzerland, 2013.
57. *ISO 25178-2:2012*; Geometrical Product Specifications (GPS)—Surface Texture: Areal—Part 2: Terms, Definitions and Surface Texture Parameters. Polski Komitet Normalizacyjny, Wydział Wydawnictw Normalizacyjnych: Warszawa, Poland, 2014.
58. Peker, O.; Bolgul, B. Evaluation of surface roughness and color changes of restorative materials used with different polishing procedures in pediatric dentistry. *J. Clin. Pediatr. Dent.* **2023**, *47*, 72–79. [CrossRef]
59. Alqahtani, A.S.; Al-Qutobi, I.A.; Al-Shammari, K.F.; Almutairi, A.; Al-Rabiah, A. Comparison of marginal integrity and surface roughness of CoCr copings fabricated by different fabrication techniques. *Appl. Sci.* **2021**, *11*, 8328. [CrossRef]
60. Lima, F.G.; Romano, A.R.; Correa, M.B.; Demarco, F.F. Influence of microleakage, surface roughness and biofilm control on secondary caries formation around composite resin restorations: An in-situ evaluation. *J. Appl. Oral Sci.* **2009**, *17*, 61–65. [CrossRef]
61. Shih, W.-Y. Microleakage in different primary tooth restorations. *J. Chin. Med. Assoc.* **2016**, *79*, 228–234. [CrossRef]
62. Karadaş, M.; Demirbuğa, S. Evaluation of color stability and surface roughness of bulk-fill resin composites and nanocomposites. *Meandros Med. Dent. J.* **2017**, *18*, 199–205. [CrossRef]
63. Bhadra, D.; Shah, N.C.; Rao, A.S.; Dedania, M.S.; Bajpai, N. A 1-year comparative evaluation of clinical performance of nanohybrid composite with activa bioactive composite in class ıı carious lesion: A randomized control study. *J. Conserv. Dent.* **2019**, *22*, 92–96. [CrossRef]
64. Fraga, M.A.A.; Correr-Sobrinho, L.; Sinhoreti, M.A.C.; Carletti, T.M.; Correr, A.B. Do dual-cure bulk-fill resin composites reduce gaps and improve depth of cure. *Braz. Dent. J.* **2021**, *32*, 77–86. [CrossRef]
65. Wang, R.; Liu, H.; Wang, Y. Different depth-related polymerization kinetics of dual-cure, bulk-fill composites. *Dent. Mater.* **2019**, *35*, 1095–1103. [CrossRef] [PubMed]
66. Ortengren, U.; Wellendorf, H.; Karlsson, S.; Ruyter, I.E. Water sorption and solubility of dental composites and identification of monomers released in an aqueous environment. *J. Oral Rehabil.* **2001**, *28*, 1106–1115. [CrossRef] [PubMed]
67. Yamanel, K. Effect of different prophylactic polishing procedures on the surface roughness of microhybrid and nanohybrid resin composites. *Cumhur. Dent. J.* **2018**, *21*, 85–92. [CrossRef]

68. Güner, Z.; Köse, H.D. Evaluation of nanohardness, elastic modulus, and surface roughness of fluoride-releasing tooth-colored restorative materials. *J. Clin. Pediatr. Dent.* **2024**, *48*, 131–137. [CrossRef] [PubMed]
69. Sajini, S.I.; Mushayt, A.B.; Almutairi, T.A.; Abuljadayel, R. Color stability of bioactive restorative materials after immersion in various media. *J. Int. Soc. Prev. Community Dent.* **2022**, *12*, 418–425. [CrossRef]
70. Da Mata, M.; Santos-Pinto, L.; Cilense Zuanon, A.C. Influences of the insertion method in glass ionomer cement porosity. *Microsc. Res. Tech.* **2012**, *75*, 667–670. [CrossRef]
71. Al Zangana, T.; Tuygunov, N.; Yahya, N.A.; Aziz, A.A. The impact of resin coatings on the properties and performance of glass ionomer cements: A systematic review. *J. Mech. Behav. Biomed. Mater.* **2025**, *169*, 107044. [CrossRef] [PubMed]
72. Kanik, Ö.; Turkun, L.S.; Dasch, W. In vitro abrasion of resin-coated highly viscous glass ionomer cements: A confocal laser scanning microscopy study. *Clin. Oral Investig.* **2017**, *21*, 821–829. [CrossRef]
73. Ugurlu, M. How do the surface coating and one-year water aging affect the properties of fluoride-releasing restorative materials? *Niger. J. Clin. Pract.* **2020**, *23*, 720–728. [CrossRef]
74. Patel, B.; Chhabra, N.; Jain, D. Effect of different polishing systems on the surface roughness of nano-hybrid composites. *J. Conserv. Dent.* **2016**, *19*, 37–40. [CrossRef] [PubMed] [PubMed Central]
75. Bollen, C.M.L.; Lambrechts, P.; Quirynen, M. Comparison of Surface Roughness of Oral Hard Materials to the Threshold Surface Roughness for Bacterial Plaque Retention: A Review of the Literature. *Dent. Mater.* **1997**, *13*, 258–269. [CrossRef]
76. Gehrke, P.; Dinkel, J.; Fischer, C.; Schmenger, K.; Sader, R. Surface Roughness and Necessity of Manual Refinishing Requirements of CAD/CAM-Manufactured Titanium and Cobalt-Chrome Bars—A Pilot Study. *Open Dent. J.* **2019**, *13*, 316–326. [CrossRef]
77. Buchenau, T.; Mertens, T.; Lohner, H.; Bruening, H.; Amkreutz, M. Comparison of optical and stylus methods for surface texture characterisation in industrial quality assurance of post-processed laser metal additive Ti-6Al-4V. *Materials* **2023**, *16*, 4815. [CrossRef]
78. Adamczak, S.; Świderski, J.; Stępień, K.; Dobrowolski, T.; Chmielik, I.P. Comparative analysis of surface roughness measurements obtained with the use of contact stylus profilometry and coherence scanning interferometry. In Proceedings of the XXI IMEKO World Congress Measurement in Research and Industry, Prague, Czech Republic, 30 August 2015. Available online: https://www.imeko.org/publications/wc-2015/IMEKO-WC-2015-TC14-316.pdf (accessed on 25 December 2025).
79. Ruzova, T.A.; Haddadi, B. Surface roughness and its measurement methods—Analytical review. *Results Surf. Interfaces* **2025**, *19*, 100441. [CrossRef]
80. Raszewski, Z.; Brząkalski, D.; Derpeński, Ł.; Jałbrzykowski, M.; Przekop, R.E. Aspects and Principles of Material Connections in Restorative Dentistry-A Comprehensive Review. *Materials* **2022**, *15*, 7131. [CrossRef] [PubMed] [PubMed Central]
81. Bourgi, R.; Kharouf, N.; Cuevas-Suárez, C.E.; Lukomska-Szymanska, M.; Haikel, Y.; Hardan, L. A Literature Review of Adhesive Systems in Dentistry: Key Components and Their Clinical Applications. *Appl. Sci.* **2024**, *14*, 8111. [CrossRef]

Disclaimer/Publisher's Note: The statements, opinions and data contained in all publications are solely those of the individual author(s) and contributor(s) and not of MDPI and/or the editor(s). MDPI and/or the editor(s) disclaim responsibility for any injury to people or property resulting from any ideas, methods, instructions or products referred to in the content.